Journal of Catalysis 263 (2009) 83–91

Contents lists available at ScienceDirect

Journal of Catalysis

www.elsevier.com/locate/jcat

Activation of dimethyl gold complexes on MgO for CO oxidation: Removal of methyl ligands and formation of catalytically active gold clusters

Yalin Hao, Bruce C. Gates *

Department of Chemical Engineering and Materials Science, University of California, Davis, CA 95616, USA

ARTICLE INFO

Article history:
Received 13 November 2008
Revised 26 January 2009
Accepted 26 January 2009
Available online 13 February 2009

Keywords:
Organo-gold complex
Gold catalyst
MgO
IR
CO oxidation
X-ray absorption spectroscopy

ABSTRACT

A supported CO oxidation catalyst was synthesized by the reaction of $Au(CH_3)_2(acac)$ (acac is acetylacetonate) with partially dehydroxylated MgO powder. The as-prepared sample was found by infrared (IR) and extended X-ray absorption fine structure (EXAFS) spectroscopies to incorporate dimethyl gold complexes that were bonded to the support; it lacked measurable catalytic activity for CO oxidation at room temperature. As the temperature was increased to >373 K with the sample in flowing $CO + O_2$ at atmospheric pressure, removal of methyl ligands from the gold was observed by IR and EXAFS spectroscopies. Simultaneously, the sample became active for CO oxidation catalysis. EXAFS characterization of the sample right after the activation indicated that the gold had aggregated into clusters consisting of approximately 4–6 Au atoms each, on average. These are among the smallest supported gold clusters yet reported, and they are inferred to be the catalytically active species. The XANES data suggest that the gold in the activated catalyst had not been reduced to the metallic state.

1. Introduction

Highly dispersed supported gold catalysts have attracted wide interest because of their high activities and selectivities for reactions including low-temperature oxidation of CO [1], epoxidation of propylene [2], oxidation of unsaturated ketones [3], and hydrogenation of nitro compounds [4]. Notwithstanding extensive research on supported gold catalysts, fundamental questions remain, such as what are the catalytically active sites and reaction mechanisms, even for the most thoroughly investigated reaction, CO oxidation [5,6].

The performance of supported gold catalysts for CO oxidation is sensitive to the catalyst precursor and preparation method [7], the support [8], pretreatment conditions [9], and water content of the reactant mixture [10]. Halides, commonly used in catalyst precursors (e.g., $HAuCl_4$) also affect the catalyst performance. For example, chloride caused aggregation of the gold during synthesis and pretreatment of supported catalysts, and it also poisoned them [5].

To avoid components such as chloride, we used an organometallic precursor, $Au(CH_3)_2(acac)$ (acac is acetylacetonate, $C_5H_7O_2$) [11–23]. Because it is highly volatile (with a sublimation point of approximately 298 K), $Au(CH_3)_2(acac)$ can be transferred as a vapor at temperatures close to room temperature and thus deposited readily onto almost all kinds of supports [12,14,15]; catalysts have also been prepared from this precursor by adsorption onto supports from hydrocarbon solutions [13,22,23].

The ligands on the supported gold species formed from $Au(CH_3)_2(acac)$ can be removed at low temperatures, affording catalysts with extremely high gold dispersions, even including catalysts incorporating mononuclear gold complexes [13,16,17], which can be readily converted into gold clusters [11,14]. In most cases, the supported mononuclear gold samples prepared from $Au(CH_3)_2(acac)$ have initially retained the methyl ligands of the precursor [13,16–18]. Some of these complexes have evidently been the physisorbed precursor itself [18], and some have been chemisorbed, with the acac ligands being replaced by oxygen atoms of the support (which acts as a bidentate ligand) [13,16,17].

The supported gold complexes have for the most part not been found to be active for CO oxidation—because of retention of the organic ligands on the gold [19]. Treatments to remove some of the ligands have been reported, such as calcination in air at temperatures $\geqslant$473 K [19], and treatment in helium at temperatures $\geqslant$573 K [17]. The resultant (activated) catalysts have typically been found to contain reduced and aggregated gold, with average gold cluster diameters commonly being $\geqslant$15 Å, as evidenced by transmission electron microscopy (TEM) images and extended X-ray absorption fine structure (EXAFS) spectra [17,19]. For example, Guzman et al. [20] reported that gold particles of ap-

* Corresponding author.
E-mail address: bcgates@ucdaivs.edu (B.C. Gates).

0021-9517/$ – see front matter
doi:10.1016/j.jcat.2009.01.015

proximately 30 Å in average diameter formed on MgO, giving a catalyst that was active and stable for CO oxidation at room temperature.

There are a few reports of catalytic activity for CO oxidation attributed to supported mononuclear gold complexes themselves (in contrast to gold clusters). For example, Au(III) complexes on zeolite NaY were reported to catalyze CO oxidation, and EXAFS spectra indicated the lack of gold clusters in the used catalyst [18]. In this sample, the $Au(CH_3)_2(acac)$ precursor was initially physisorbed on the support [18]. The methyl ligands were readily removed from the Au atoms by evacuation at room temperature (but the gas-phase products were not identified) [23]; in contrast, higher decomposition temperatures (exceeding 353 K) were observed for other chemisorbed gold complexes prepared similarly on various metal oxides [11]. Infrared (IR) spectra of adsorbed CO indicated the presence of mononuclear Au(III) species on zeolite NaY initially during CO oxidation catalysis at room temperature, and during subsequent operation of the catalyst in a flow reactor the Au(III) was reduced to Au(I) (with no EXAFS evidence of aggregation of the gold), accompanied by a decline in the catalytic activity by an order of magnitude [18]. MgO-supported mononuclear gold complexes were also reported to be active for ethylene hydrogenation at 353 K [22].

Notwithstanding the work on supported mononuclear gold complexes and gold clusters with average diameters in the range of 15–50 Å, there is a lack of information about the structures and catalytic behavior of extremely small supported gold clusters (those with average diameters less than about 15 Å), except for (A) investigations carried out with clusters deposited from the vapor phase and characterized under ultrahigh-vacuum conditions [24] and (B) investigations showing increases of catalytic activity with the growth of gold clusters, which we discuss below and extend in this work.

By using $Au(CH_3)_2(acac)$ as a precursor and controlling the degree of aggregation of the gold on the support (MgO powder), we have been able to investigate the genesis of a CO oxidation catalyst containing extremely small gold clusters as a result of activation by removal of methyl ligands from the supported gold complex. The catalyst was tested in a flow reactor at atmospheric pressure. By using IR and EXAFS spectroscopies to characterize the catalyst in the working state, we have shown that the gold became catalytically active at room temperature when the methyl groups were removed from the gold and the gold was simultaneously converted into clusters consisting of 4–6 Au atoms each, on average.

2. Experimental

2.1. Materials

Helium (Airgas, 99.995%) and CO (Airgas, 10% in He, 99.999%) were purified by passage through traps containing reduced Cu/Al_2O_3 and activated zeolite 4A to remove traces of O_2 and moisture, respectively. O_2 (Airgas, 10% in He, 99.999%) was purified by passage through a trap containing activated zeolite 4A to removed traces of moisture. The MgO powder support (EM Science, 97%, 60 m^2/g) was partially dehydroxylated by calcination in O_2 at 673 K for 2 h (the temperature was chosen for consistency with the work of Guzman et al. [13,20], who used the same precursor and support), followed by evacuation at 673 K for 16 h (pressure $< 10^{-2}$ Pa), and stored in an argon-filled glove box until it was used. *n*-Pentane solvent (Fisher, 99%) was dried and purified by refluxing over sodium metal and deoxygenated by sparging of N_2. The catalyst precursor $Au(CH_3)_2(acac)$ (Strem, 98%, handled as light- and temperature-sensitive) was used as supplied.

2.2. Sample preparation

The synthesis and handling of MgO-supported gold samples were carried out with exclusion of air and moisture on a double-manifold Schlenk vacuum line and in the glove box. Samples were prepared by slurrying $Au(CH_3)_2(acac)$ in dried and deoxygenated *n*-pentane with MgO at 298 K and 10^5 Pa. The slurry was stirred for 1 day, and the solvent was removed by evacuation for 1 day (pressure $< 10^{-2}$ Pa), giving a sample containing 1.0 wt% Au, which was stored in the glove box until used.

2.3. CO oxidation catalysis and product analysis by mass spectrometry (MS)

Calcined MgO alone and the as-prepared sample consisting of mononuclear Au(III) complexes bonded to the support [13] were tested separately for CO oxidation catalysis, as the reaction temperature was ramped from room temperature to 573 K at 3 K/min. The sample (typically, 0.20 g) was loaded into a once-through plug-flow reactor in the glove box and transferred to a flow system without coming in contact with air. The partial pressures of the components in the reactant stream (Pa) were $P_{CO} = 1520$, $P_{O_2} = 1520$, and $P_{He} = 9.83 \times 10^4$. The total feed gas flow rate was 100 mL (NTP) min^{-1}.

In other experiments, the as-prepared Au/MgO sample was first treated in flowing $CO + O_2$ as the temperature increased from room temperature to 408 K at 3 K/min and then cooled to 303 K in flowing helium to start the CO oxidation reaction. The component partial pressures (Pa) were $P_{CO} = 760$, $P_{O_2} = 760$, and $P_{He} = 1.00 \times 10^5$. The total gas feed flow rate was always 100 mL (NTP) min^{-1}.

During the treatments mentioned above and during CO oxidation catalysis, the effluent gases from the reactor were analyzed by mass spectrometry. The on-line instrument was a Balzers OmniStar running in multi-ion monitoring mode. Signals were recorded for the main fragments of CO ($m/e = 28$); O_2 ($m/e = 32$); CO_2 ($m/e = 44$); and CH_3 ($m/e = 15$). Signals are reported relative to that of the helium carrier gas ($m/e = 4$) to remove effects of small pressure fluctuations during the experiments.

2.4. IR spectroscopy

Transmission IR spectra of the as-prepared catalyst sample were recorded with a Bruker IFS 66v spectrometer operated with a spectral resolution of 2 cm^{-1}; each reported spectrum is an average of 16 scans. Samples were pressed into self-supporting wafers and loaded into a cell (In situ Research Instruments, South Bend, IN) in the glove box. The cell allowed recording of spectra as treatment gases flowed through and around the wafer at temperatures ranging from room temperature to 573 K.

In the IR experiments, the initially prepared sample was treated in a flowing mixture of CO and O_2 as the temperature increased from room temperature to 408 K at 3 K/min. The total flow rate was 100 mL (NTP) min^{-1} with CO and O_2 partial pressures of 760 Pa each (and the remainder helium).

2.5. X-ray absorption spectroscopy

Characterization of catalyst samples by X-ray absorption spectroscopy was carried out in transmission mode at beam line X-18B at the National Synchrotron Light Source (NSLS) at Brookhaven National Laboratory (BNL), Upton, NY. The storage ring electron energy was 2.8 GeV; the ring current varied within the range of 140–300 mA.

The powder sample was loaded into a cell [25] that allowed collection of data characterizing catalysts in reactive atmospheres.

Table 1
Crystallographic data characterizing the reference compounds and Fourier transform ranges used in the EXAFS analysis.[a]

Reference compound	Shell	Crystallographic data			Fourier transformation	
		N	R (Å)	Ref.	Δk (Å^{-1})	Δr (Å)
Gold foil	Au–Au	12	2.88	[29]	1.00–20.00	0.00–8.00
$Au(CH_3)_2(acac)$	Au–O	1	1.99	[30]	1.00–20.00	0.00–8.00
$Au(CH_3)_2(acac)$	Au–C	1	2.07	[30]	1.00–20.00	0.00–8.00
$IrMg_3$	Ir–Mg	1	2.62	[31]	1.00–20.00	0.00–8.00

[a] Notation: N, coordination number; R, distance between absorber and backscatterer atoms; Δk and Δr, intervals used in the Fourier transformation.

EXAFS spectra of the sample in flowing helium were determined at room temperature (four scans were recorded). The sample mass was chosen to give an absorbance of 2.5 at the Au L_{III} edge (11919 eV); to allow determination of a proper energy calibration, a gold foil was scanned simultaneously with the sample.

XANES spectra were then recorded after the composition of the flowing mixture was changed to include $CO + O_2$ (the CO and O_2 partial pressures were 760 Pa each, and the remainder was helium). With this now reactive feed mixture, the cell was heated to 408 K at 3 K/min and then cooled to room temperature, followed by purging with helium; XANES spectra were recorded periodically during the whole operation. Then another four EXAFS scans were recorded with the sample in flowing helium at room temperature.

3. EXAFS data analysis

Analysis of the EXAFS data recorded at the Au L_{III} edge was carried out with a difference file technique by use of the software XDAP [26]. The number of parameters used in fitting the data was justified statistically by the Nyquist theorem: $n = (2\Delta k \Delta r/\pi) + 1$, where Δk and Δr, respectively, are the ranges in k and r used in the data fitting (k is the photoelectron wave vector; r is the distance from the absorber Au atom) [27]. Criteria used to judge the appropriateness of a model tested in the data fitting were that both the magnitude and imaginary part of the Fourier-transformed data fit well with both k^1 and k^3 weightings of the data.

The models considered in the fitting included Au–Au contributions (both first- and second-shell contributions), Au–C, and Au–support contributions (Au–O and Au–Mg). Reference files incorporating amplitude- and phase-shift functions characteristic of the various EXAFS contributions were obtained from theoretical calculations by use of the software FEFF [28] (Table 1). For example, the reference for the Au–Au contribution was generated with FEFF7 from crystallographic data characterizing metallic gold; the reference for the Au–Mg contribution was generated with FEFF7 from crystallographic data characterizing $IrMg_3$ (the transferability of the amplitude- and phase-shift functions from neighboring atoms in the periodic table has been justified experimentally [32]). The amplitude reduction factor [33] was determined to be 0.92 by fitting the spectrum of gold foil by using the FEFF-generated reference for gold metal; this value was used in the analyses of the spectra of the supported samples.

Because the amplitude–shift functions characteristic of the Au–C and Au–O contributions are transferable, it is difficult to distinguish one of these contributions from the other in the data analysis.

Various candidate models were used to determine fits representing the MgO-supported gold sample before and after the treatment in flowing $CO + O_2$ at 408 K. Details of these candidate models and the diagnostic parameters characterizing the best fit with each are summarized in the Supplemental information. Only the models that fit the data best with physically realistic parameters are presented here (Table 2).

Table 2
EXAFS results at the Au L_{III} edge characterizing MgO-supported gold species formed by adsorption of $Au(CH_3)_2(acac)$ on MgO (a) before CO oxidation catalysis ($\Delta k = 3.98$–12 Å^{-1}, $\Delta r = 1$–3 Å) and (b) after CO oxidation catalysis ($\Delta k = 3.92$–12.96 Å^{-1}, $\Delta r = 1$–4 Å).[a]

Sample	Shell	N	R (Å)	$10^3 \times \Delta\sigma^2$ (Å^2)	ΔE_0 (eV)
Catalyst before CO oxidation reaction	Au–C	1.8	1.97	2.8	−4.4
	Au–O	2.1	2.09	1.6	−4.4
Catalyst after CO oxidation reaction	Au–C	1.1	1.92	2.1	0.4
	Au–O	1.7	2.03	3.2	0.4
	Au–Mg[b]	0.3	2.48	2.4	−4.8
	Au–Au	3.1	2.81	9.9	1.9
	Au–Mg[b]	0.3	3.65	1.5	−4.8

[a] Notation: N, coordination number; R, distance between absorber and backscatterer atoms; $\Delta\sigma^2$, relative Debye–Waller factor; ΔE_0, inner potential correction. The accuracies are estimated to be as follows: N, ±10% for Au-high-Z contributions and ±20% for Au-low-Z contributions; R, ±0.02 Å; $\Delta\sigma^2$, ±20%; and ΔE_0, ±20% [35].

[b] This contribution is too small to allow a confident assignment. It was included to make the overall fitting complete.

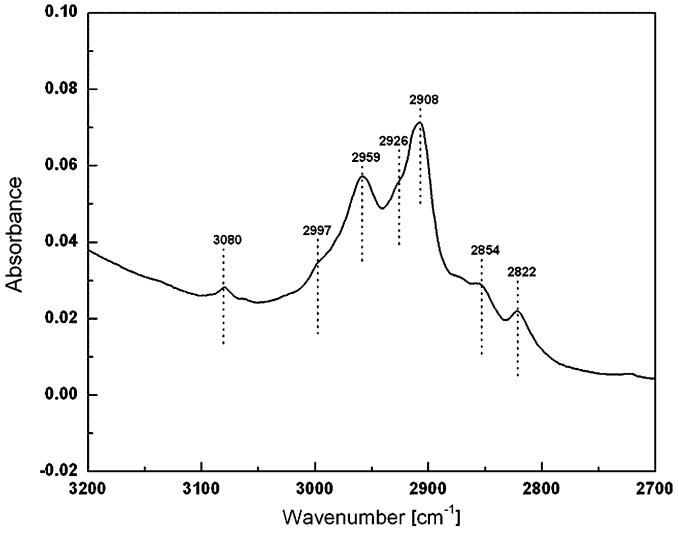

Fig. 1. IR spectrum of the sample formed by reaction of $Au(CH_3)_2(acac)$ with partially dehydroxylated MgO in the C–H stretching region (3200–2700 cm^{-1}).

4. Results

4.1. Structural characterization of dimethyl gold complexes supported on MgO

The results obtained with the samples reported here confirm those reported by Guzman et al. [34], who used the same precursor and support. The IR peaks in the $\nu_{(C-H)}$ region (Fig. 1), including those at 3080, 2997, 2959, 2926, 2908, 2854, and 2822 cm^{-1} (Fig. 1), characterize $\nu_{(C-H)}$ modes representative of methyl and acac groups. The bands at 2959 and 2908 cm^{-1} were assigned [34] to the asymmetric and symmetric stretching modes of Au–CH_3, indicating that the methyl ligands were still bonded to the gold after adsorption of the precursor. The peaks in the $\nu_{(C-C)}$, $\nu_{(C-O)}$, and $\nu_{(O-H)}$ stretching regions (spectra not shown) were also consistent with the report of Guzman et al. [34], indicating that the acac ligands were displaced from the gold to form both Hacac and Mg(acac) species on the support [34].

The EXAFS data characterizing the supported gold sample in flowing helium at room temperature give no evidence of Au–Au contributions, consistent with the inference that the supported gold species were site-isolated and mononuclear (Table 2). Each Au atom, on average, was bonded to two carbon atoms at the distance of 1.97 Å (Table 2, Fig. 2), confirming that the methyl lig-

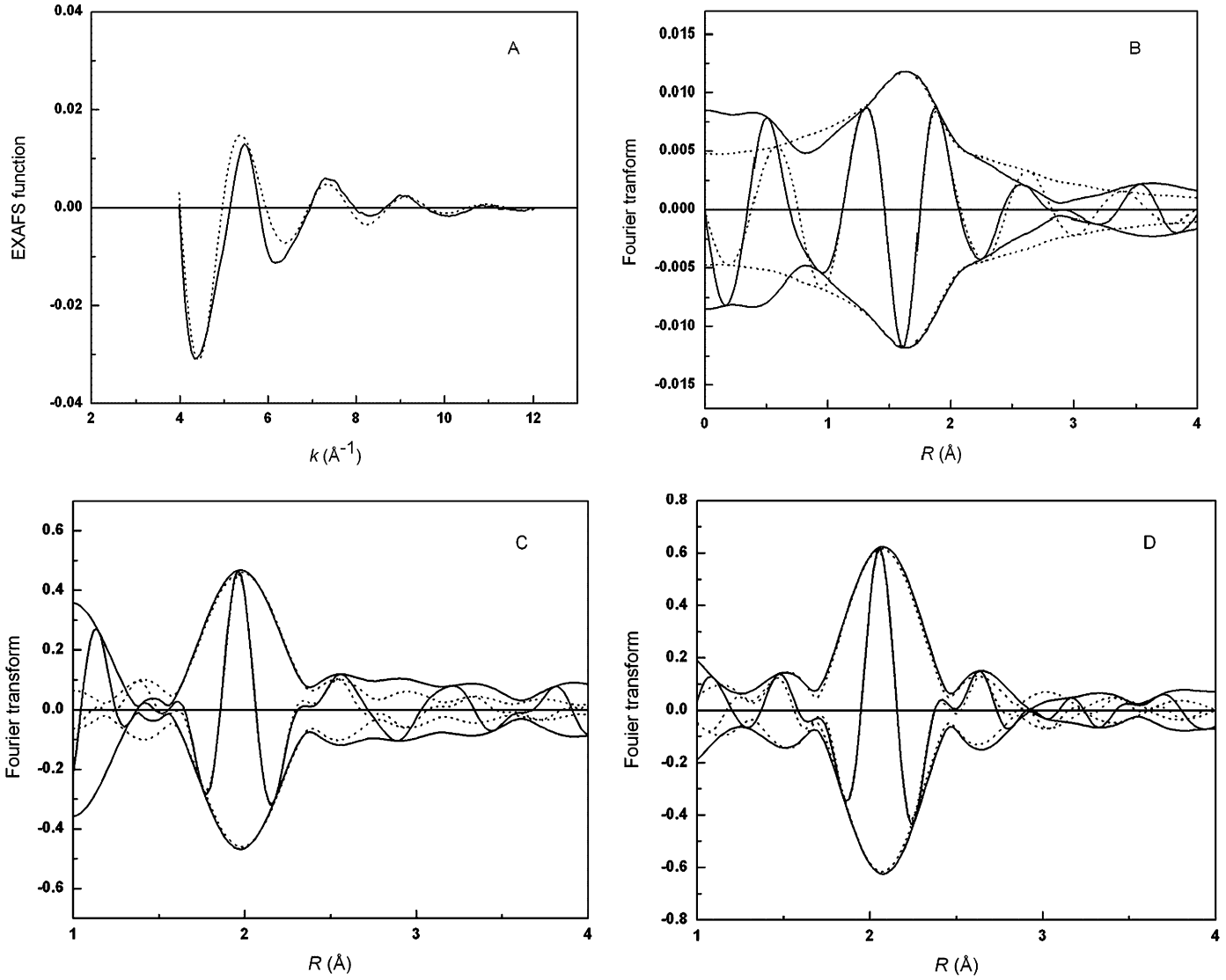

Fig. 2. Results of EXAFS analysis characterizing sample made from $Au(CH_3)_2(acac)$ and partially dehydroxylated MgO: (A) experimental EXAFS function (solid line) and sum of the calculated Au–C + Au–O contributions (dotted line); (B) imaginary part and magnitude of uncorrected Fourier transform (k^0-weighted) of experimental EXAFS function (solid line) and sum of the Au–C + Au–O contributions (dotted line); (C) residual spectrum illustrating the Au–C contribution: imaginary part and magnitude of corrected Fourier transform (k^1-weighted) of experimental results minus the calculated Au–O contribution (solid line) and, for comparison, the calculated Au–C contribution (dotted line); (D) residual spectrum illustrating the Au–O contribution: imaginary part and magnitude of corrected Fourier transform (k^1-weighted) of experimental results minus the calculated Au–C contribution (solid line) and, for comparison, the calculated Au–O contribution (dotted line).

ands were retained on the gold. Moreover, the EXAFS data (Table 2, Fig. 2) show that each Au atom, on average, was bonded to approximately two oxygen atoms, as evidenced by the Au–O contribution at 2.09 Å with a coordination number of 2.1[1]; these were assigned to oxygen atoms of the MgO support, as acac ligands had been displaced from the gold.

In summary, both the IR and EXAFS data are consistent with the inference that the as-prepared gold sample contained mononuclear dimethyl gold complexes incorporating two oxygen atoms of the support, which was a bidentate ligand. Thus, the structure of the supported gold complex is analogous to that of the precursor $Au(CH_3)_2(acac)$ [20], in which the acac ligand is bidentate, the gold is formally Au(III), and the metal complex is coordinatively saturated.

4.2. Temperature-programmed CO oxidation catalyzed by MgO-supported gold

The initially prepared sample evidenced no detectable catalytic activity for CO oxidation at 303 K under the conditions investigated ($P_{CO} = 1520$, $P_{O_2} = 1520$, and $P_{He} = 9.83 \times 10^4$ Pa). As the temperature was increased to >373 K, an increase was observed in the mass spectral signal $m/e = 15$ (Fig. 3). Similarly, this signal had been observed during the temperature-programmed decomposition of the sample in flowing helium [36], and the gas-phase products were identified as methane, ethane, and ethylene [36], evidently formed from the methyl ligands bonded to the gold. We thus infer that the supported mononuclear Au(III) species in $CO + O_2$ started to decompose at 373 K.

[1] Both the Au–C and Au–O distances (Table 2) are 0.07 Å shorter than those determined by Guzman and Gates [13], and the difference between his result and ours cannot be explained solely by the EXAFS analysis errors (±0.02 Å). A likely explanation for the difference is that the reference files used by us and by Guzman et al. were different. We used theoretical references calculated on the basis of crystallographic data characterizing $Au(CH_3)_2(acac)$, whereas Guzman and Gates used experimental references obtained from EXAFS spectra of $Au(CH_3)_2(acac)$ [22].

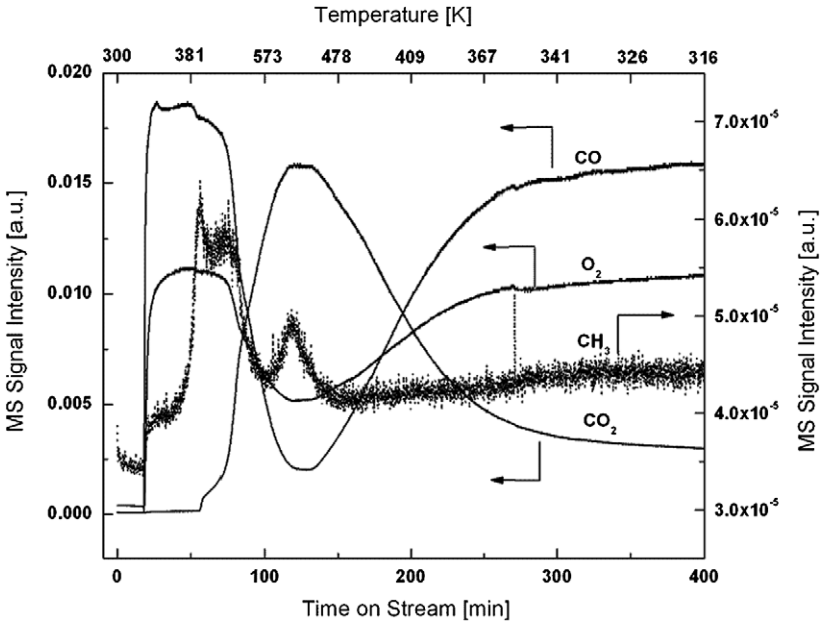

Fig. 3. Changes in intensity of the mass spectral signals of the effluent gases from the flow reactor during CO oxidation catalysis as the temperature was first increased from room temperature to 573 K at 3 K/min and then cooled to 303 K. The reactor contained 0.2 g of MgO-supported gold formed by the reaction of $Au(CH_3)_2(acac)$ with partially dehydroxylated MgO.

The intensity of the mass spectral signal $m/e = 15$ reached a maximum at 393 K (Fig. 3) (a second peak appeared at a higher temperature, possibly caused by the decomposition of the acac ligands on the support [11]), and, simultaneously, the supported gold sample became active for CO oxidation, as indicated by the increase in intensity (from the baseline value) of the mass spectral signal $m/e = 44$ representing CO_2 (Fig. 3). As the temperature was increased further, to 573 K, the catalytic activity continued to increase (Fig. 3): the conversion of CO at 573 K reached roughly 90%, a value much higher than that observed when the reaction was catalyzed by the MgO support alone at the same temperature (approximately 15%). A third peak represented by the mass spectral signal $m/e = 15$ also appeared at approximately 573 K, indicating the decomposition of some surface species formed during the treatment. These species could have been the products of acac decomposition. However, there is not yet enough evidence to determine either their structures or their locations.

When the temperature of the now activated catalyst was subsequently lowered to 303 K, the production of CO_2 decreased (Fig. 3), but the supported gold sample was still catalytically active (the CO conversion was approximately 4%) at 303 K; the MgO support itself did not show any measurable catalytic activity for CO oxidation.

4.3. Structural characterization of activated catalyst

After the experiment described above was finished, the color of the catalyst had changed to purple (it was initially white), consistent with the formation of gold clusters [37]. We were motivated to investigate the samples after activation under only the mildest conditions, because then we expected the catalyst to incorporate only the smallest gold clusters [11].

Thus, we treated a sample in the initially prepared state in flowing $CO + O_2$ as the temperature was ramped up to only 408 K, the approximate temperature at which the onset of catalytic activity was observed (Fig. 3). Structural changes of the sample during the heating to 408 K (at $P_{CO} = 760$, $P_{O_2} = 760$, and $P_{He} = 1.0 \times 10^4$ Pa) were followed by IR and X-ray absorption spectroscopies. Details of the characterization results follow in the next sections.

4.3.1. Removal of methyl ligands from gold

After CO and O_2 had been introduced into the stream flowing through the IR cell, the removal of methyl groups from the gold at room temperature was evidenced by small decreases in the intensities of the $\nu_{(C-H)}$ stretching bands at 2960, 2902, and 2817 cm^{-1} (Fig. 4A). Corresponding changes that would have been expected in the mass spectral signal at $m/e = 15$ (indicative of light alkanes) were too small to be observed at this temperature (Fig. 3), but, as the temperature was increased to 378 K, the IR band intensities decreased markedly (Fig. 4A), indicating that the process was accelerated, and the mass spectral signal $m/e = 15$ correspondingly increased in intensity (Fig. 3), demonstrating the conversion of the methyl groups into light alkanes.

The EXAFS data confirm the removal of methyl ligands from the gold during the treatment. After the sample had been activated in $CO + O_2$ at 408 K, the removal of the methyl ligands was less than complete, however, as evidenced by the decrease of the Au–C coordination number only from 1.8 to 1.1 (Table 2).

We recognize that Au–C contributions could have arisen from species such as carbonates formed during the catalytic reaction of CO and O_2 [36]. The IR spectra (Fig. 4B) show that indeed carbonate-like species (carbonates, bicarbonates, carboxylates, and/or formates) did form on the catalyst, even at temperatures as low as room temperature. However, the frequencies of the bands (approximately 1660, 1500, and 1380 cm^{-1}) demonstrate that these carbonate-like species were bonded to the MgO rather than to the gold [36].

Nonetheless, there is evidence that carbonate-like species did form on the gold. As removal of methyl ligands became evident in the IR spectra at temperatures exceeding 378 K (consistent with the appearance of light alkanes shown by the mass spectra of the effluent gas), weak bands arose at 1618 and 1523 cm^{-1} (Fig. 4B); these have been attributed to carbonate-like species on gold [36].

Because carbonates and the related species are negatively charged, we infer that positively charged species must have been present on the catalyst surface where these anionic species were bonded. This inference suggests a possible role of cationic gold sites in the CO oxidation catalysis, which might include cationic

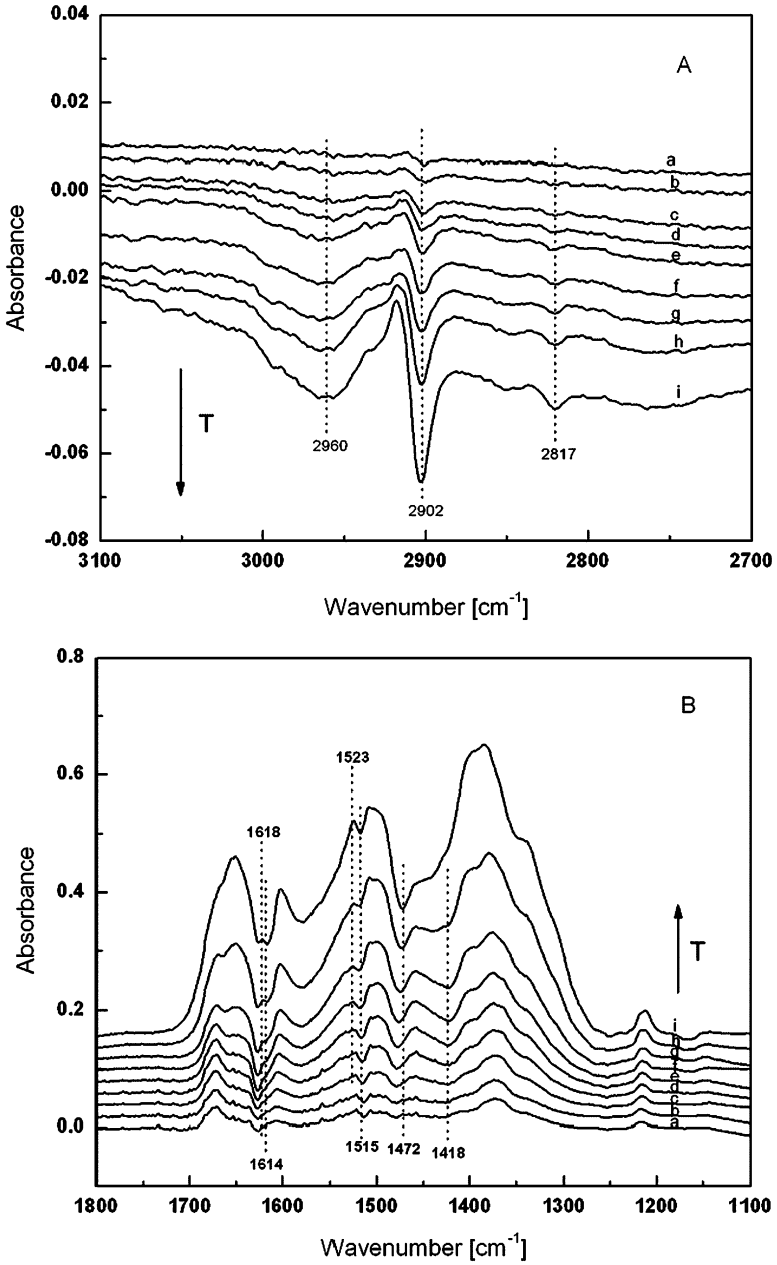

Fig. 4. Changes in the difference IR spectra in (A) 3100–2700 cm^{-1} region and (B) 1800–1100 cm^{-1} region when the sample made from $Au(CH_3)_2(acac)$ and partially dehydroxylated MgO was treated under conditions of CO oxidation catalysis as the temperature was ramped from room temperature to 408 K at 3 K/min: (a) spectrum recorded at room temperature 5 min after start of flow of $CO + O_2$, followed by spectra recorded at the following temperatures (K): (b) 303; (c) 318; (d) 333; (e) 348; (f) 363; (g) 378; (h) 398; and (i) 408.

species in association with gold clusters [36], such as gold cations at the metal–support interface.

4.4. Evidence of reduction of gold as it underwent aggregation

The activation of the gold during the heating to 408 K in flowing $CO + O_2$ was further characterized by XANES spectroscopy. XANES spectra at the Au L_{III} edge characteristic of Au(III) species (exemplified by $Au(CH_3)_2(acac)$) typically include an intense peak (the white line, Supplemental Information, Fig. 1) at an energy approximately 4 eV higher than the absorption edge, corresponding to the excitation of a $2p_{3/2}$ electron to the empty *d* state. In contrast, the XANES data representing zerovalent gold species (gold foil) are characterized by the absence of this white line (Supplemental Information, Fig. 1).

The XANES spectrum of the initially prepared sample in the presence of flowing helium at room temperature is characterized by features that essentially match those of $Au(CH_3)_2(acac)$ (Fig. 5A), indicating that the formal oxidation state of the gold in the supported sample was +3. Immediately after the start of flow of $CO + O_2$ into the X-ray absorption spectroscopy cell containing the catalyst, a slight change in the XANES spectrum was observed, as the intensity of the white line at the Au L_{III} edge declined, consistent with the onset of reduction of the gold (Figs. 5A and 5B). The white-line intensity decreased continuously as the temperature increased to 408 K. No further change in this intensity was observed as the sample was cooled in $CO + O_2$ and purged with helium at room temperature. The XANES spectrum after the treatment was still markedly different from that of metallic gold (Fig. 5A), suggesting that the sample contained a substantial proportion of cationic gold.

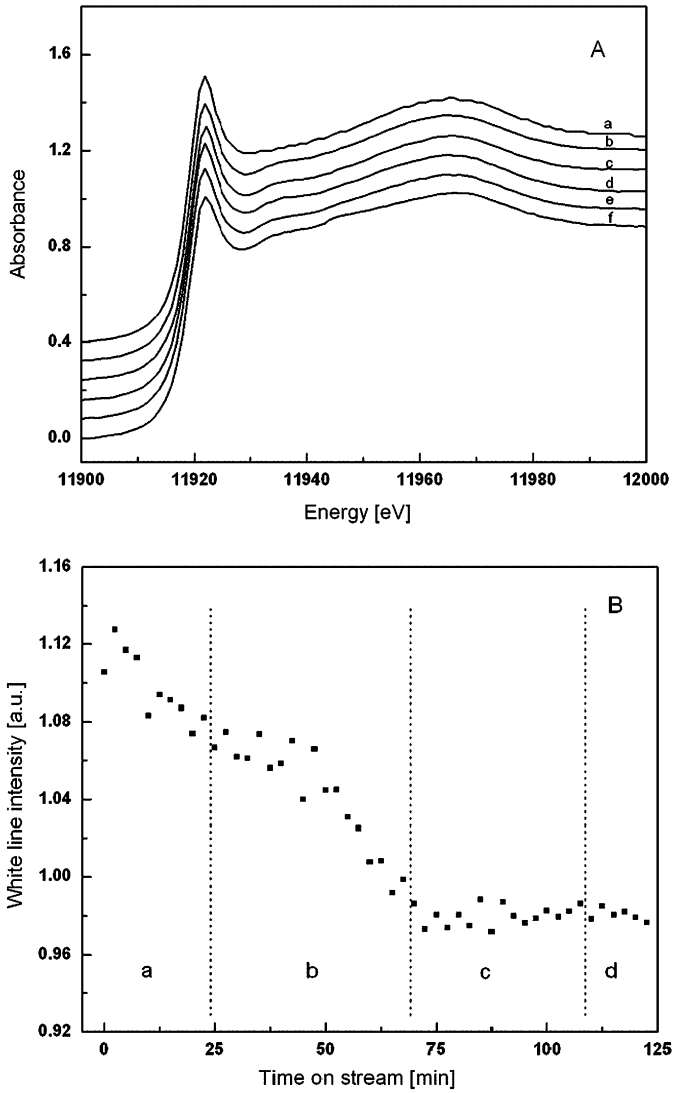

Fig. 5. (A) XANES spectra recorded when the sample synthesized from $Au(CH_3)_2(acac)$ and partially dehydroxylated MgO was treated under conditions of CO oxidation catalysis at increasing temperatures: spectra recorded (a) at room temperature right after start of flow of $CO + O_2$ flow; (b) at room temperature 30 min after start of flow of $CO + O_2$; and then at the following temperatures (K): (c) 310; (d) 340; (e) 370; and (f) 400. (B) Changes in white-line intensities during the consecutive treatments: during CO oxidation catalysis (a) at room temperature; (b) as the temperature was ramped from room temperature to 408 K at 3 K/min; (c) as the temperature was ramped from 408 K to room temperature; and (d) as the sample thereafter was purged with helium at room temperature.

EXAFS data characterizing the sample after the treatment in $CO + O_2$ at 408 K also provide evidence that the gold had undergone aggregation. The EXAFS data (Table 2) indicate an Au–Au contribution at 2.80 Å with a coordination number of 3.1, corresponding to gold clusters with only 4–6 Au atoms each, on average [38]. As the removal of methyl ligands was not complete at this temperature (Fig. 3, Table 2), the sample is inferred to have contained a mixture of gold species, presumably including unconverted mononuclear Au(III) species along with the clusters indicated by the Au–Au coordination number.

In summary, during the activation of the MgO-supported gold catalyst in $CO + O_2$, removal of methyl ligands took place, accompanied by aggregation of the gold, as some reduction of the gold occurred. The sample formed at this early stage of activation contained gold clusters incorporating, on average, only 4–6 Au atoms each.

4.5. Catalytic activity of the sample treated at 408 K in flowing $CO + O_2$

The sample that had been treated in flowing $CO + O_2$ at 408 K was found to be active at 303 K (Fig. 6). A near-steady state was reached in the catalyst performance in less than 1 h on stream, with the CO conversion being roughly 0.7% under the conditions stated in Section 2. The catalyst was stable for more than 20 h of continuous operation in the flow reactor. The calculated number of turnovers (CO_2 molecules formed per Au atom) was approximately 250.

5. Discussion

$Au(CH_3)_2(acac)$ is a precursor that reacts readily with metal oxides, including MgO, to make dimethyl gold(III) complexes on the oxide surface [13,16,17]—methyl groups are retained on the gold. Removal of methyl ligands from the gold at elevated temperatures in $CO + O_2$ led to the genesis of an active catalyst for CO oxidation (Fig. 3). The EXAFS and XANES data respectively show that the removal of the methyl groups was associated with the onset of aggregation and reduction of the gold (Figs. 5A and 5B, Table 2). However, the gold catalyst formed initially (after the initial stage of the catalyst activation) was still characterized by an Au–C contribution (Table 2), in addition to the Au–Au contribution, consistent with the inference that this sample (containing extremely small clusters) still contained some mononuclear gold species that incorporated methyl ligands. The IR (Fig. 4A) and mass spectrometry (Fig. 3) data support this inference.

XANES spectra show a slight reduction of the gold during the initial stage of catalyst activation (Fig. 5A). This result is consistent with the formation of extremely small gold clusters indicated by the Au–Au contribution in the EXAFS data (Table 2): a coordination number of 3.1 corresponds to gold clusters with approximately 4 Au atoms each, on average. Because the XANES spectrum of this initially activated sample (Fig. 5A, spectrum f) still shows a strong white line, we infer that the small gold clusters are likely to be cationic. Indeed, theoretical calculations carried out by Siloco et al. [39] confirm that small cationic gold clusters are stable on MgO. This conclusion is contrasted with that of Yang et al. [40], who suggested that there were separate phases incorporating mononuclear Au^{3+} species, on the one hand, and Au^0 clusters, on the other, in their the TiO_2-supported catalyst that was activated in a way similar to ours. They inferred that the activation of their catalyst was associated with the reduction of mononuclear $AuO_x(OH)^-_{4-2x}$ species to metallic gold. We hypothesize that, in agreement with Yang et al. [40], that the gold complexes had activities that were negligible relative to the observed activity, which is attributed to the gold clusters present with them. However, there is not sufficient evidence in our judgment to support the inference that extremely small supported gold clusters were metallic.

Some authors have observed that mononuclear gold complexes on supports are themselves active for CO oxidation catalysis [18,41], and to test the possibility that such complexes in our samples were active would require that we control the removal of the methyl ligands to obtain mononuclear gold complexes with reduced numbers of these ligands—without the formation of gold clusters. The data show that we were not able to do this—the clusters formed rapidly upon removal of the methyl ligands, and this result suggests that mononuclear gold species on the MgO surface migrated rapidly and combined with other gold species, removing the coordinative unsaturation generated by removal of methyl groups by formation of Au–Au bonds instead. We would expect the rapid migration of the gold complexes to have been facilitated by hydroxyl groups on the support surface (they were indicated by IR spectra of the sample in the O–H stretching region). Support for the suggestion is provided by reports indicating

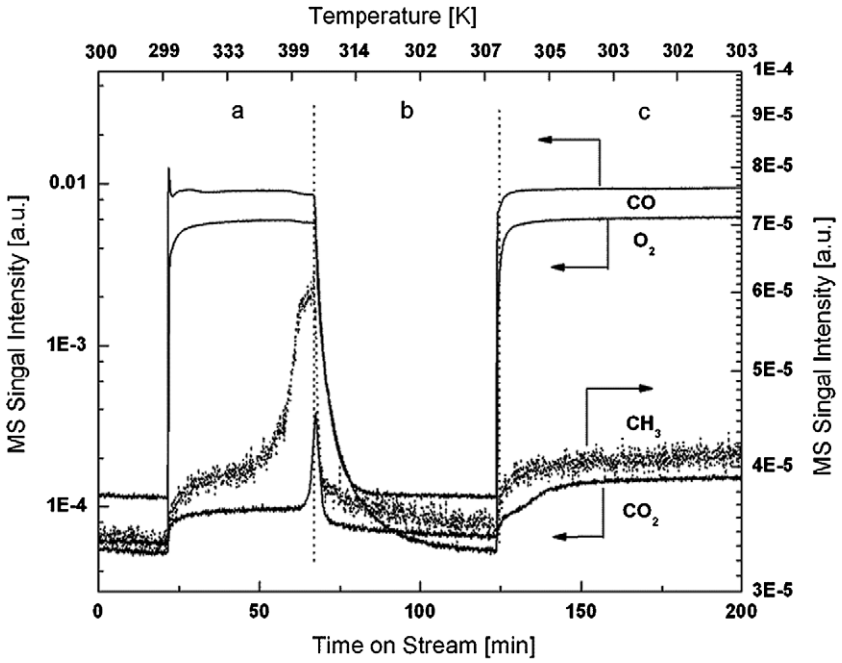

Fig. 6. Changes in intensities of the mass spectral signals of the effluent gases from the flow reactor containing the sample synthesized from $Au(CH_3)_2(acac)$ and partially dehydroxylated MgO as the sample underwent the following treatments: (a) CO oxidation catalysis as the temperature increased from room temperature to 408 K at 3 K/min; (b) subsequent purging of the sample with helium as the temperature was ramped down to room temperature; and (c) during CO oxidation catalysis at room temperature.

that hydroxyl groups on SiO_2, MgO, and γ-Al_2O_3 facilitate the migration of rhodium carbonyl species [42].

In contrast to our observations, Aguilar-Guerrero and Gates [41] observed that mononuclear gold species on CeO_2 were active for CO oxidation catalysis. Their samples were made from the same precursor as ours and by a similar preparation method, but a mononuclear gold complex (indicated by EXAFS spectroscopy) remained stable on the CeO_2 support for 2 h during CO oxidation catalysis at 353 K. EXAFS characterization of the mononuclear sample after 2 h of CO oxidation catalysis in a flow reactor at 353 K included an Au–C contribution with a coordination number of approximately 2 at the distance of 2.13 Å (the Au–C distance was 2.05 Å in the initially prepared sample), although methyl groups had been removed from the gold (as evidenced by the IR spectrum of the sample [43]). The Au–C contribution was thus ascribed to the carbonate-like species formed on the gold.

The stability of a mononuclear gold species on CeO_2, in contrast to the lack of its stability on our hydroxylated MgO, might be attributed (a) to the lack of hydroxyl groups on the CeO_2 surface after gold deposition, as evidenced by the IR spectrum of the sample in the O–H stretching region [43], and/or (b) to the presence of oxygen vacancies on the CeO_2, demonstrated by various microscopic characterizations [44]. The MgO surface is also expected to have incorporated some vacancies, but the concentration of vacancies on MgO, which depends on the calcination temperature [45], is expected to have been much less than on CeO_2 at our calcination temperature.

The gold in the CeO_2-supported sample started to aggregate after 2 h of CO oxidation catalysis, accompanied by an increase in the catalytic activity comparable to that observed in our work. Thus, small gold clusters on CeO_2 were demonstrated to be more active than the mononuclear gold species, consistent with our results. In this respect, the cited results are in agreement with ours, and we suggest that the inference that small gold clusters are more active for CO oxidation than mononuclear gold complexes result is general, independent of the support.

Thus, a key result of our work and that of Aguilar-Guerrero and Gates [41] is that extremely small gold clusters are active for CO oxidation catalysis, even at room temperature. The activity of the CeO_2-supported gold clusters is comparable to those of some of the more highly active gold catalysts that have been reported [5], although the average diameter of these gold clusters (approximately 7 Å) [41] was much less than that proposed by Valden et al. [46] and Bamwenda et al. [47] to be the optimum gold cluster diameter (25–30 Å). On the other hand, Herzing et al. [48] recently proposed that the presence of bilayers of gold incorporating approximately 10 Au atoms (with a diameter of about 5 Å) led to the high catalytic activity of an iron oxide-supported gold sample; the dimension of these bilayers is comparable to that of the clusters observed by Aguilar-Guerrero and Gates [41].

We emphasize that mixtures of gold clusters with various diameters existed in most of the supported gold catalysts that have been investigated. Thus, it still seems to be premature to draw conclusions about the optimum gold cluster size.

The work presented here indicates how to prepare supported gold clusters that contain only a few atoms each under practical conditions, in contrast to the laser vaporization methods that have been used under ultra-high vacuum conditions [49–51]. Samples such as ours and others [41], containing clusters of only a few Au atoms and/or mononuclear Au(III) species, seem to be important both for the opportunities they offer for fundamental understanding of the size- and structure-dependency of catalysis by gold [52] and also for the opportunities they may offer for preparation of catalysts with new properties—properties in the blurry zone linking molecular and nanoscale structures [53–55].

In summary, removal of methyl ligands from gold was required to activate the MgO-supported gold sample prepared by reaction of $Au(CH_3)_2(acac)$ with partially hydroxylated MgO. Synthesis of supported gold catalysts with this precursor offers us the ability to prepare extremely small gold clusters by control over the treatment conditions, which provides the opportunity to investigate these clusters under non-vacuum conditions.

6. Conclusions

We investigated the activation of an MgO-supported gold catalyst for CO oxidation that was prepared by the reaction of

$Au(CH_3)_2(acac)$ with the partially dehydroxylated support. The catalyst activation results from the removal of methyl ligands from the gold, accompanied by the formation of gold clusters containing only a few atoms each. The onset of catalytic activity does not require that the gold be reduced to the metallic state.

Acknowledgments

We thank Professor Juan Carlos Fierro-Gonzalez for helpful discussions. This work was supported by US Department of Energy, Office of Energy Research, Office of Basic Energy Sciences (Grant FG02-04ER15513). We also acknowledge the National Synchrotron Light Source (NSLS), Brookhaven National Laboratory, beam line X-18B, for access to beam time; the NSLS is supported by the US Department of Energy, Office of Science, Basic Energy Sciences, under Contract No. DE-AC02-98CH10886. We thank the beam line staff for assistance.

Supplementary Information

The online version of this article contains additional supplementary information, including EXAFS and XANES data and details of the EXAFS analysis.

Please visit DOI: 10.1016/j.jcat.2009.01.015.

References

[1] M. Haruta, S. Tsubota, T. Kobayashi, H. Kageyama, M.J. Genet, B. Delmon, J. Catal. 144 (1993) 175.
[2] B. Chowdhury, J.J. Bravo-Suárez, M. Daté, S. Tsubota, M. Haruta, Angew. Chem. Int. Ed. 45 (2006) 412.
[3] C. Milone, R. Ingoglia, L. Schipilliti, C. Crisafulli, G. Neri, S. Galvagno, J. Catal. 236 (2005) 80.
[4] A. Corma, Science 313 (2006) 332.
[5] M.C. Kung, R.J. Davis, H.H. Kung, J. Phys. Chem. C 111 (2007) 11767, and references cited therein.
[6] G.C. Bond, D.T. Thompson, Gold Bull. 33 (2000) 41.
[7] G.R. Bamwenda, S. Tsubota, T. Nakamura, M. Haruta, Catal. Lett. 44 (1997) 83.
[8] M.M. Schubert, S. Hackenberg, A.C. van Veen, M. Muhler, V. Plzak, R.J. Behm, J. Catal. 197 (2001) 113.
[9] F. Boccuzzi, A. Chiorino, M. Manzoli, P. Lu, T. Akita, S. Ichikawa, M. Haruta, J. Catal. 202 (2001) 256.
[10] M. Daté, M. Okumura, S. Tsubota, M. Haruta, Angew. Chem. Int. Ed. 43 (2004) 2129.
[11] J.C. Fierro-Gonzalez, Y. Hao, B.C. Gates, J. Phys. Chem. C 111 (2007) 6645, and references cited therein.
[12] M. Okumura, S. Nakamura, S. Tsubota, T. Nakamura, M. Azuma, M. Haruta, Catal. Lett. 51 (1998) 53.
[13] J. Guzman, B.C. Gates, Angew. Chem. Int. Ed. 42 (2003) 690.
[14] M. Haruta, Gold Bull. 37 (2004) 27, and references therein.
[15] M. Okumura, S. Tsubota, M. Haruta, J. Mol. Catal. A 199 (2003) 73.
[16] J. Guzman, B.C. Gates, Langmuir 19 (2003) 3897.
[17] J. Guzman, S. Kuba, J.C. Fierro-Gonzalez, B.C. Gates, Catal. Lett. 95 (2004) 77.
[18] J.C. Fierro-Gonzalez, B.C. Gates, J. Phys. Chem. B 108 (2004) 16999.
[19] M. Okumura, K. Tanaka, A. Ueda, M. Haruta, Solid State Ionics 95 (1997) 143.
[20] J. Guzman, B.C. Gates, J. Phys. Chem. B 106 (2002) 7659.
[21] M. Okumura, M. Haruta, Chem. Lett. 29 (2000) 396.
[22] J. Guzman, B.C. Gates, J. Catal. 226 (2004) 111; J. Guzman, B.C. Gates, Angew. Chem. Int. Ed. 42 (2003) 690.
[23] M. Mihaylov, J.C. Fierro-Gonzalez, H. Knözinger, B.C. Gates, K. Hadjiivanov, J. Phys. Chem. B 110 (2006) 7695.
[24] U. Landman, B. Yoon, C. Zhang, U. Heiz, M. Arenz, Top. Catal. 44 (2007) 145, and references cited therein.
[25] J.F. Odzak, A.M. Argo, F.S. Lai, B.C. Gates, K. Pandya, L. Feraria, Rev. Sci. Instr. 72 (2001) 3943.
[26] M. Vaarkamp, J.C. Linders, D.C. Koningsberger, Physica B 209 (1995) 159.
[27] E.A. Stern, Phys. Rev. B 48 (1993) 9825.
[28] A.L. Ankudinov, J.J. Rehr, Phys. Rev. B 56 (1997) R1712.
[29] P. Villars, L.D. Calvert, Pearson's Handbook of Crystallographic Data for Intermetallic Phases, vol. 1, ASM International, Materials Park, OH, 1991, p. 1260.
[30] M. Trömel, E.D.Z. Lupprich, Anorg. Allg. Chem. 414 (1975) 160.
[31] P. Villars, L.D. Calvert, Pearson's Handbook of Crystallographic Data for Intermetallic Phases, vol. 4, ASM International, Materials Park, OH, 1991, p. 4106.
[32] F.B.M. Duivenvoorden, D.C. Koningsberger, Y.S. Uh, B.C. Gates, J. Am. Chem. Soc. 108 (1986) 6254.
[33] D.C. Koningsberger, B.L. Mojet, G.E. van Dorssen, D.E. Ramaker, Top. Catal. 10 (2000) 143.
[34] J. Guzman, B.G. Anderson, C.P. Vinod, K. Ramesh, J.W. Niemantsverdriet, B.C. Gates, Langmuir 21 (2005) 3675.
[35] O. Alexeev, B.C. Gates, Top. Catal. 10 (2000) 273.
[36] Y. Hao, M. Mihaylov, E. Ivanova, K. Hadjiivanov, H. Knözinger, B.C. Gates, J. Catal. 261 (2009) 137.
[37] S. Galvano, G. Parravano, J. Catal. 55 (1978) 178.
[38] A. Jentys, Phys. Chem. Chem. Phys. 1 (1999) 4059.
[39] S. Sicolo, C. Di Velentin, G. Pacchioni, J. Phys. Chem. C 111 (2007) 5154.
[40] J.F. Yang, J.D. Henao, M.C. Raphulu, Y. Wang, T. Caputo, A.J. Groszek, M.C. Kung, M.S. Scurrell, J.T. Miller, H.H. Kung, J. Phys. Chem. B 109 (2005) 10319.
[41] V. Aguilar-Guerrero, B.C. Gates, Chem. Commun. (2007) 3210.
[42] J.-M. Basset, F. Lefebvre, C. Santini, Coord. Chem. Rev. 178–180 (1998) 1703.
[43] V. Aguilar-Guerrero, private communication, 2008.
[44] H. Nörenberg, G.A.D. Briggs, Phys. Rev. Lett. 79 (1997) 4222.
[45] T. Karasuda, K.-i. Aika, Bull. Chem. Soc. Jpn. 71 (1998) 1999.
[46] M. Valden, X. Lai, D.W. Goodman, Science 281 (1998) 1647.
[47] G.R. Bamwenda, S. Tsubota, T. Nakamura, M. Haruta, Catal. Lett. 44 (1997) 83.
[48] A.A. Herzing, C.J. Kiely, A.F. Carley, P. Landon, G.J. Hutchings, Science 321 (2008) 1331.
[49] S. Lee, C. Fan, T. Wu, S.L.J. Anderson, Chem. Phys. 123 (2005) 124710.
[50] X. Tong, L. Benz, P. Kemper, H. Metiu, M.T. Bowers, S.K. Buratto, J. Am. Chem. Soc. 127 (2005) 13516.
[51] S. Lee, C. Fan, T. Wu, S.L. Anderson, J. Am. Chem. Soc. 126 (2004) 5682.
[52] M. Haruta, Chem. Rec. 3 (2003) 75.
[53] A. Corma, H. Garcia, Chem. Soc. Rev. 37 (2008) 2096.
[54] J.C. Fierro-Gonzalez, B.C. Gates, Chem. Soc. Rev. 37 (2008) 2127.
[55] B.C. Gates, Nat. Nanotechnol. 3 (2008) 583.